

This discussion paper is/has been under review for the journal Atmospheric Chemistry and Physics (ACP). Please refer to the corresponding final paper in ACP if available.

Horizontal divergence of typhoon-generated gravity waves in the upper troposphere and lower stratosphere (UTLS) and its influence on typhoon evolution

S. H. Kim¹, H.-Y. Chun², and W. Jang²

¹Center of Excellence in Earth Systems Modeling and Observations, Chapman University, Orange, CA, USA

²Department of Atmospheric Sciences, Yonsei University, Seoul, Korea

Received: 14 February 2013 – Accepted: 20 October 2013 – Published: 6 November 2013

Correspondence to: H.-Y. Chun (chunhy@yonsei.ac.kr)

Published by Copernicus Publications on behalf of the European Geosciences Union.

Title Page

Abstract

Introduction

Conclusions

References

Tables

Figures

◀

▶

◀

▶

Back

Close

Full Screen / Esc

Printer-friendly Version

Interactive Discussion

Abstract

The characteristics of horizontal divergence induced by typhoon-generated gravity waves (HDTGW) and the influence of HDTGW on typhoon evolution are investigated based on the simulation results of Typhoon Saomai (2006) using the Weather Research and Forecasting (WRF) model. The power spectral density of HDTGW shows dominant powers at horizontal wavelengths of 20–30 km and at periods of less than one hour. This is associated with gravity waves generated by vigorous convective clouds in an inner core region of the typhoon. However, the domain-averaged HDTGW in the upper troposphere and lower stratosphere had a spectral peak at 24 h, which is well correlated with the minimum sea-level pressure of the typhoon, especially during a rapidly developing period. The 24 h period of the averaged HDTGW stems from the inertia-gravity waves generated by the convective clouds in the spiral rainbands, and showed no clear association with the thermal tides or the diurnal variation of precipitation.

1 Introduction

A typhoon consists of strong convective clouds having various spatiotemporal scales, which can generate inertia-gravity waves (IGWs) that reach to the stratosphere. Several observational (e.g., Dhaka et al., 2003; Chun et al., 2007) and numerical modeling (e.g., Kim et al., 2005; Kuester et al., 2008; Kim and Chun, 2010, 2011) studies have investigated the characteristics of vertically propagating gravity waves generated by the convective clouds associated with typhoons. Among these studies, Kim et al. (2005) showed that typhoon-generated gravity waves (TGWs) could be an important source of the momentum budget in the middle atmosphere. Eastward-propagating TGWs in the summer hemisphere that survive into the upper stratosphere and mesosphere in easterly background winds can transport the positive momentum in the summer hemisphere required to maintain the wind and temperature in the middle atmosphere general circulation.

ACPD

13, 28953–28972, 2013

Horizontal divergence of typhoon-generated gravity waves

S. H. Kim et al.

Title Page

Abstract

Introduction

Conclusions

References

Tables

Figures

◀

▶

Back

Close

Full Screen / Esc

Printer-friendly Version

Interactive Discussion



Recently Kim and Chun (2011; KC11 hereafter) investigated the effects of TGWs on the environmental flows of a typhoon by examining changes in the vertical wind shear and horizontal divergence in the upper troposphere and lower stratosphere (UTLS). Based on a simulation of Typhoon Saomai (2006), they showed that TGWs contribute significantly to the upper-level horizontal divergence near the typhoon center, with relatively less contribution to the vertical wind shear. The effects of upper-level divergence on the evolution of typhoons have been investigated in several previous studies (e.g., Merrill, 1988; Bosart et al., 2000; Rappin et al., 2011). Among these, Rappin et al. (2011) showed that a typhoon can be intensified by reducing resistance of the upper-level outflow associated with the secondary circulation of typhoon convection based on the Carnot theory of the maximum potential intensity (Emanuel, 1986). They suggested that typhoon outflow weakens the environmental inertial stability, even under the upper-level jet, which minimizes the energy expended in developing and expanding the outflow, and allows for more energy to be utilized for typhoon intensification.

Considering that horizontal divergence in the upper troposphere is one of the major dynamic factors determining surface pressure tendency (Holton, 1992), and that TGWs contribute significantly to horizontal divergence during typhoon evolution, there may be feedback between TGWs and their sources. The objective of this study is to understand this feedback process precisely. To do so, we examine the characteristics of the horizontal divergence of TGWs (HDTGWs) in the UTLS, and their contribution to typhoon evolution based on the WRF model-simulated results of Typhoon Saomai (2006) that was reported by Kim and Chun (2010; KC10 hereafter).

2 Numerical experiment

The numerical model used for this study is the Advanced Research Weather Research and Forecasting (WRF-ARW) model version 2.2. The simulations used three domains (D1, D2, and D3, hereafter) with horizontal grid spacings of 27 km (D1), 9 km (D2), and 3 km (D3). The number of horizontal grid points is 187×187 , 253×253 , and 397×397 for

Horizontal divergence of typhoon-generated gravity waves

S. H. Kim et al.

[Title Page](#)

[Abstract](#)

[Introduction](#)

[Conclusions](#)

[References](#)

[Tables](#)

[Figures](#)

◀

▶

◀

▶

[Back](#)

[Close](#)

[Full Screen / Esc](#)

[Printer-friendly Version](#)

[Interactive Discussion](#)



Title Page	
Abstract	Introduction
Conclusions	References
Tables	Figures
◀	▶
◀	▶
Back	Close
Full Screen / Esc	
Printer-friendly Version	
Interactive Discussion	

D1, D2, and D3, respectively. The center of D1 is at 20° N and 128° E. The model employed two-way nesting with an innermost domain (D3) designed to follow the typhoon center. Seventy-seven vertical levels were used from the surface to 5 hPa ($z = \sim 35$ km) with a damping layer at the uppermost 5 km. The resultant physical domain ranged from the surface to $z = \sim 30$ km, with a vertical grid spacing of ~ 500 m in the troposphere. D1 and D2 were integrated over 60 h (from 06:00 UTC 8 August to 18:00 UTC 10 August) and D3 was integrated over 54 h from 12:00 UTC 8 August. Details in the simulation can be found in KC10. To avoid unrealistic signals while the vortex was spinning up and to focus on the rapid development and decay stages of Typhoon Saomai, the results from the 48 h between 12:00 UTC 8 and 12:00 UTC 10 were selected and are presented in this study.

3 Results

3.1 Domain-averaged HDTGWs in the upper troposphere

To examine the characteristics of upper-level divergence from the TGWs, components satisfying the frequency range of IGWs ($f^2 < \hat{\omega}^2 < N^2$, where f is the Coriolis parameter, $\hat{\omega}$ ($\equiv \omega - U k - V l$) is the intrinsic frequency, where ω is the ground-based frequency, U and V are the domain-averaged zonal and meridional winds, and k and l are the zonal and meridional wavenumbers, respectively, and N is the Brunt–Vaisala frequency) were extracted from the total divergence fields at each vertical level. One of the interesting findings reported in KC11 is that the domain-averaged HDTGWs in D3 showed alternating positive and negative signs with a period of about 18 h. Although no spectral analysis of the HDTGWs was performed in KC11, this result is somewhat unexpected because the dominant spectral peak of the TGWs shown in the vertical velocity of KC10 was less than one hour. In order to examine this discrepancy, we performed spectral analyses of the HDTGWs with respect to time and space.

Figure 1a shows time-height cross section of the domain-averaged HDTGWs in D3 from 12 km to 18 km above ground level (a.g.l.) (Fig. 1a). The time series of the minimum sea level pressure (SLP), domain-averaged total divergence, domain-averaged HDTGW at 16 km a.g.l. (Fig. 1b), and domain-averaged vertical velocity averaged from 5 3 km to 15 km a.g.l., and domain-averaged 30 min accumulated precipitation amount (Fig. 1c) are also included. Shown in Fig. 1e is the power spectral density (PSD) of HDTGW with respect to frequency at several selected heights. Figure 1a reveals that HDTGWs in the upper troposphere show a periodic divergence and convergence pattern, especially over 13.5 km a.g.l. The magnitude of the divergence and convergence is 10 larger when the typhoon is intensifying (from 17:00 UTC 8 to 17:00 UTC 9), because intense convection accompanying the typhoon generates large amplitude gravity waves.

The domain-averaged total divergence (Fig. 1b) is positive in most times except for few hours near 20:00 UTC 9 at which the minimum SLP starts to increase. There is a significant correlation between the total divergence and HDTGW throughout the entire 48 h period, except in a decaying period after 00:00 UTC 10. During a rapidly developing 12 h period (00:00 UTC to 12:00 UTC 9) in which the minimum SLP drops from 15 966 to 938.5 hPa, the total divergence and HDTGW is strongly correlated. During this period, IGWs contribute to the total divergence about 30 % in UTLS. In this period, there is also a strong correlation between the minimum SLP and HDTGW as well as the minimum SLP and total divergence at 16 km a.g.l. The horizontal divergence/convergence that is vertically integrated from the surface to top of the atmosphere (model top in 20 this case) can determine the surface pressure tendency in a hydrostatic atmosphere (Holton, 1992). The time-height cross section of domain-averaged total divergence (not shown) denotes that the magnitude of the divergence in UTLS is much larger than that of the convergence/divergence in the troposphere, and thus temporal variation in the 25 vertically integrated divergence/convergence is largely determined by that in the divergence in UTLS. Strong correlations between the total divergence and minimum SLP, HDTGW and minimum SLP, and total divergence and HDTGW in UTLS during the rapidly developing period demonstrate the contribution of IGWs to typhoon evolution.

[Title Page](#)[Abstract](#)[Introduction](#)[Conclusions](#)[References](#)[Tables](#)[Figures](#)[◀](#)[▶](#)[Back](#)[Close](#)[Full Screen / Esc](#)[Printer-friendly Version](#)[Interactive Discussion](#)

The domain-averaged vertical velocity averaged over 3–15 km a.g.l. and domain-averaged 30 min accumulated precipitation amount (Fig. 1c) is generally well matched throughout the whole 48 h, except in a decaying period after 00:00 UTC 10. Due to the interaction of typhoon and topography, the vertical wind and precipitation increase after 5 12:00 UTC 9 and produce another peaks around 00:00 UTC 10 when outer rainbands reach Taiwan, as shown recently by Jang and Chun (2013). Correlation between the vertical velocity and HDTGW at 16 km a.g.l. varies with time. Before 17:00 UTC 8 and after 17:00 UTC 9, there is a positive relation between the two variables, while in the developing period (17:00 UTC 8–17:00 UTC 9), there is a clear negative correlation, 10 most significantly during the rapidly developing period near 01:00 UTC 9–12:00 UTC 9.

The strong negative correlation between the two variables during the rapidly developing period is somewhat unexpected. In order to understand this result, we calculated time-height cross-section of the vertical mass transport (Fig. 1d) that is the sum of the upward mass transport and downward mass transport in D3, which are the domain 15 sum of the positive and negative ρw (where ρ is the air density and w is the vertical velocity) in each grids, respectively. It shows that the total divergence and HDTGW at 16 km a.g.l. are positively correlated with the vertical transport in UTLS (9–16 km a.g.l.), while they are negatively correlated with the vertical transport below 9 km. When we check the upward mass transport and downward mass transport separately, it is found 20 that significant upward mass transport exists in the entire troposphere during the rapidly developing period, while strong downward transport exists at the same time in the lower layer. Considering that the D3 domain covers a rather wide area ($1191 \text{ km} \times 1191 \text{ km}$), as shown in Fig. 2, the downward motions occupied in relatively wider areas outside of 25 the eyewall in the lower troposphere can contribute to the negative domain-averaged vertical velocity, while upward motion occupied in relatively wider areas of anvil clouds in the upper troposphere contribute to the positive domain-averaged vertical velocity in UTLS. The correlation between the HDTGW and precipitation is generally similar to that between the HDTGW and vertical velocity.

Horizontal divergence of typhoon-generated gravity waves

S. H. Kim et al.

[Title Page](#)

[Abstract](#)

[Introduction](#)

[Conclusions](#)

[References](#)

[Tables](#)

[Figures](#)

◀

▶

[Back](#)

[Close](#)

[Full Screen / Esc](#)

[Printer-friendly Version](#)

[Interactive Discussion](#)

The PSD of HDTGWs (Fig. 1e) is largest at 15 km a.g.l., and decreases rapidly below and above 15 km a.g.l. The primary spectral peak is at $1.16 \times 10^{-5} \text{ s}^{-1}$ (with a period of about 24 h) and the secondary spectral peak is at $1.7 \times 10^{-5} \text{ s}^{-1}$ (with a period of about 16 h) for most heights. The primary and secondary peaks satisfy a 95 % confidence level. The best-track data of Typhoon Saomai from the Japan Meteorological Agency (JMA) shows that Saomai propagated to the northwest during the early stage, but stayed on a west-northwest path during our analysis period (see Fig. 1 of KC10). The latitudinal change in the typhoon track during the analysis period is from 22 to 27° N, and the corresponding inertial periods range from 32 to 26 h. This suggests that the dominant spectral peak of the HDTGW shown in Fig. 1e is near the inertial frequency.

Although the 24 h period in the HDTGW is within the frequency range of the IGWs, this variation could be related to diurnal effects, such as thermal tidal oscillation and daily rainfall variation. For the thermal tide to contribute to the present HDTGW variation, a semi-diurnal signal with even stronger power should also appear in the power spectrum of the HDTGW (Browner et al., 1977; Kossin, 2002; Yoshioka et al., 2005). However, the spectral powers near 12 h ($2.3 \times 10^{-5} \text{ s}^{-1}$) are nearly at a minimum for all heights (Fig. 1e). If the convective activity in Typhoon Saomai is associated with diurnal variation of precipitation, the solar-synchronous component can be linked to the HDTGW indirectly. In the present simulation, maximum precipitation occurred around 18:00 LST, which differs from the findings of a previous study by Jiang et al. (2011), who showed precipitation maxima in the early morning and minima in the evening using 12 yr of satellite data. Our analyses suggest that the 24 h period of the domain-averaged HDTGW is not likely to be related to thermal tidal oscillation or daily rainfall variation.

25 3.2 Spatial distribution of HDTGWs

In the previous section, we found that the dominant period of the domain-averaged HDTGW is 16–24 h and that it is strongly correlated with the evolution of a typhoon. This raises two questions: (i) why do the short period wave components with the strongest

[Title Page](#)[Abstract](#)[Introduction](#)[Conclusions](#)[References](#)[Tables](#)[Figures](#)[◀](#)[▶](#)[Back](#)[Close](#)[Full Screen / Esc](#)[Printer-friendly Version](#)[Interactive Discussion](#)

Horizontal divergence of typhoon-generated gravity waves

S. H. Kim et al.

[Title Page](#)

[Abstract](#)

[Introduction](#)

[Conclusions](#)

[References](#)

[Tables](#)

[Figures](#)

◀

▶

[Back](#)

[Close](#)

[Full Screen / Esc](#)

[Printer-friendly Version](#)

[Interactive Discussion](#)

Horizontal divergence of typhoon-generated gravity waves

S. H. Kim et al.

[Title Page](#)

[Abstract](#)

[Introduction](#)

[Conclusions](#)

[References](#)

[Tables](#)

[Figures](#)

◀

▶

◀

▶

[Back](#)

[Close](#)

[Full Screen / Esc](#)

[Printer-friendly Version](#)

[Interactive Discussion](#)

azimuthal direction, which are obtained by $c = \omega / \sqrt{k^2 + l^2}$ and $\varphi = \cos^{-1}(k / \sqrt{k^2 + l^2})$, respectively.

The horizontal wavelength spectrum (Fig. 3a) shows that dominant powers exist at wavelengths of 10–40 km with a peak near 20 km for all directions. The powers in the SE directions are relatively strong, whereas those in the SW directions are relatively weak for most wavelengths, with the exception that the strongest power for wavelengths between 10 km and 20 km exists in the north-north-west (NNW: 90–135°) direction. The period spectrum (Fig. 3b) shows that dominant powers exist at periods shorter than 1 h, and similar to the wavelength spectrum, relatively strong powers exist in the SE directions and weak powers in the SW directions. The strong powers of HDTGW at horizontal wavelengths near 20 km and at periods shorter than 1 h, as shown in Fig. 3a and b, are somewhat expected, based on the vertical velocity fields reported by KC10. This suggests that high-frequency components of HDTGW have small horizontal scales, as shown in Fig. 2a, and that they tend to cancel when averaged over the domain.

3.3 Sources of domain averaged HDTGWs

It was demonstrated in the previous section that the asymmetric structure of a typhoon can yield significant differences in the HDTGW within each quadrant, especially for high-frequency signals. However, low-frequency patterns are still present, even when higher-frequency signals are stronger in some regions, and the domain-averaged HDTGWs in all four regions have a spectral peak at 24 h (not shown), as in Fig. 1a. To investigate the source of the low-frequency variation in HDTGWs, we performed spectral analyses of the convective activity in two regions separately: the inner core region of stronger convective clouds, and the outer rainbands region of wider and intermittent convective clouds.

Figure 4a shows a Hovmöller diagram of azimuthally averaged precipitable water (PW) (Fig. 4a) and horizontal and vertical wind speed (Fig. 4b) from the Typhoon Sao-

[Title Page](#)[Abstract](#)[Introduction](#)[Conclusions](#)[References](#)[Tables](#)[Figures](#)[◀](#)[▶](#)[Back](#)[Close](#)[Full Screen / Esc](#)[Printer-friendly Version](#)[Interactive Discussion](#)

Horizontal divergence of typhoon-generated gravity waves

S. H. Kim et al.

[Title Page](#)

[Abstract](#)

[Introduction](#)

[Conclusions](#)

[References](#)

[Tables](#)

[Figures](#)

◀

▶

[Back](#)

[Close](#)

[Full Screen / Esc](#)

[Printer-friendly Version](#)

[Interactive Discussion](#)



mai simulation and PSDs of PW with respect to frequency at 40 km (Fig. 4c) and 180 km (Fig. 4d) from the typhoon center. The PW contour in Fig. 4a is azimuthally averaged and represents the wavenumber 0 axisymmetric horizontal distribution of the PW from the typhoon center. Strong convective activity in the eyewall region is evidenced by a large PW value and wind speed near 30–60 km, and is especially pronounced from 06:00 UTC 9 to 12:00 UTC 10, with short period fluctuations during that time. Note that there is a minimum SLP at 12:00 UTC 9, and Saomai began to decay at 06:00 UTC 10 (Fig. 1b). Between 18:00 UTC 8 and 06:00 UTC 9, the PW is rather small, not only near the eyewall but also in the rainbands region. This is the time at which the domain-averaged HDTGW has a minimum value, (convergence) as shown in Fig. 1a. It is not very clear at this moment whether this minimum value of HDTGW is related to wave activity or wave phase. Based on the time series of HDTGW and convective sources (vertical velocity and precipitation) shown in Fig. 1 and spatial structure of HDTGW shown in Fig. 2a, however, it is likely related to preferential wave phase in the D3 domain rather than wave activity.

The power spectrum of the PW at 40 km reveals spectral peaks at 26–30 min with a 95 % confidence level (Fig. 4c). Outside of the eyewall region, the outward-propagating PW signal is well represented. This clearly exhibits that principal or secondary rainbands spiral periodically out from the center. The PSD of the PW in the rainbands region (at 180 km) has statistically significant spectral peaks at 8–20 h (Fig. 4d). This implies that the domain-averaged HDTGW is due largely to gravity waves generated by convective clouds in the rainbands with periods longer than 8 h. Although large-amplitude gravity waves generated by vigorous convection near the eyewall with periods shorter than 1 h produce much stronger divergence and convergence simultaneously in the upper troposphere, they are for the most part cancelled out during the domain-averaging process.

As in the previous section, we divided the domain into an inner core and an outer band region. A radius of 150 km was chosen for the size of the inner core based on the PW and convective activities of Typhoon Saomai (Weatherford and Gray, 1988).

Figure 5a presents the PSDs of HDTGWs at 16 km a.g.l. with respect to the horizontal phase speed (radius) and propagation direction (azimuthal angle) in the total (left), inner core (middle), and outer rainbands (right) regions of D3. The HDTGW in the inner core region is isotropic, and the dominant powers are seen at phase speeds slower than 20 ms^{-1} and mostly at about 10 ms^{-1} . The power of the HDTGW in the outer rainbands region is much weaker, with relatively strong powers in the SE and NW directions. In the SE direction, notable powers extend to higher-phase speeds (up to 40 ms^{-1}). The HDTGW PSD in the outer rainbands region results from filtering of the TGWs by background winds in the UTLS, unlike in the inner core regions where convective clouds extend to almost 16 km a.g.l. and relatively high-frequency waves propagate vertically very quickly with less filtering by background wind. In the zonal wavenumber and frequency domain, the vertical propagation of IGWs is determined by two factors: latitude that determines the Coriolis parameter and the basic-state wind structure in the target height range of wave propagation (Chun et al., 2007). The domain-averaged zonal and meridional winds change from southeasterly to northeasterly below 16 km a.g.l. (see Fig. 4 of KC10) during the time considered in the present study, which covers the azimuthal angles between $150\text{--}240^\circ$. Therefore, a large portion of TGWs in these azimuthal angles are filtered out at 16 km a.g.l. in the outer rainbands region, as revealed by the relatively weak powers in the directions of $150\text{--}270^\circ$ in Fig. 5a.

The time series of the domain-averaged HDTGWs in the inner core (Fig. 5b) shows much more irregular temporal variations compared with the total (Fig. 1a) and outer bands (Fig. 5c), mainly due to irregular temporal variations in the convective activity of the inner core region. The HDTGW in the outer bands region is strikingly similar to the total HDTGW shown in Fig. 1a. This result implies that, during the averaging process, high-frequency variation in the inner core region disappears, with only the divergence pattern in the outer rainbands region remaining. The spectral analysis of the domain-averaged HDTGW at 16 km a.g.l. with respect to the frequency reveals (not shown) that PSDs in both the total and the outer band regions have a primary peak at 24 h, with

[Title Page](#)[Abstract](#)[Introduction](#)[Conclusions](#)[References](#)[Tables](#)[Figures](#)[◀](#)[▶](#)[◀](#)[▶](#)[Back](#)[Close](#)[Full Screen / Esc](#)[Printer-friendly Version](#)[Interactive Discussion](#)

a secondary peak at about 16 h. The inner core region has relatively strong powers at several high frequencies, including a primary peak at 16 h and a secondary peak at about 3.4 h.

4 Conclusions

- In this study, the characteristics of the horizontal divergence of typhoon-generated gravity waves (HDTGWs) are examined using mesoscale simulation of typhoon Saomai and a spectral analysis method. It was found that HDTGWs show strong power in the lower stratosphere at horizontal wavelengths and periods of about 10–20 km and less than an hour, respectively, regardless of the azimuthal angle of wave propagation from the typhoon center. This is consistent with a previous study by KC10 of the vertical velocity field. However, the domain-averaged HDTGW in the typhoon center had a spectral peak at 24 h. The 24 h period of the averaged HDTGW stems from the inertia-gravity waves (IGW) generated by the relatively weak and low-frequency convective clouds in the spiral rainbands, and showed no clear association with the thermal tides or the diurnal precipitation trend. The strong HDTGW powers in the inner core region with relatively short period components are mostly filtered out during the domain-averaging process.

A time series of the domain-averaged HDTGW in the upper troposphere and lower-stratosphere (UTLS) is well correlated with the total divergence in UTLS as well as the minimum sea-level pressure (SLP) of Saomai, implying typhoon and gravity wave feedback through HDTGWs. Given that the upper-level divergence is known to have a crucial role in changes in typhoon intensity, TGWs and, more specifically, HDTGWs in the UTLS should be considered in future typhoon intensity studies, and especially in the outer rainbands region, as one of the mechanisms used to explain the temporal variation in the minimum sea-level pressure of typhoon centers.

Title Page	
Abstract	Introduction
Conclusions	References
Tables	Figures
	
Back	Close
Full Screen / Esc	
Printer-friendly Version	
Interactive Discussion	

Acknowledgements. This work was supported by the National Research Foundation of Korea (NRF) grant funded by the Korea government (MEST) (No. 20110000060 and 2013R1A2A2A01014644).

References

- 5 Bosart, L. F., Bracken, W. E., Molinari, J., Velden, C. S., and Black, P. G.: Environmental influences on the rapid intensification of Hurricane Opal (1995) over the Gulf of Mexico, Mon. Weather Rev., 128, 322–352, 2000.
- Browner, S. P., Woodley, W. L., and Griffith, C. G.: Diurnal oscillation of the area of cloudiness associated with tropical storms, Mon. Weather Rev., 105, 856–864, 1977.
- 10 Chun, H.-Y., Goh, J.-S., and Kim, Y.-H.: Characteristics of inertio-gravity waves revealed in rawinsonde data observed in Korea during 20 August to 5 September 2002, J. Geophys. Res., 112, D16108, doi:10.1029/2006JD008348, 2007.
- Dhaka, S. K., Takahashi, M., Shibagaki, Y., Yamanaka, M. D., and Fukao, S.: Gravity wave generation in the lower stratosphere due to passage of the typhoon 9426 (Orchid) observed by the MU radar at Shigaraki (34.858° N, 136.108° E), J. Geophys. Res., 108, 4595, doi:10.1029/2003JD003489, 2003.
- 15 Emanuel, A. K.: An air-sea theory for tropical cyclones, part I: Steady-state maintenance, J. Atmos. Sci., 43, 585–604, 1986.
- Holton, J. R.: An Introduction to Dynamic Meteorology, Academic Press, San Diego, USA, 20 1992.
- Jang, W. and Chun, H.-Y.: The effects of topography on the evolution of typhoon Saomai (2006) under the influence of tropical storm Bopha (2006), Mon. Weather Rev., 141, 468–489, 2013.
- Jiang, H., Liu, C., and Zipser, E. J.: A TRMM-based tropical cyclone cloud and precipitation feature database, J. Appl. Meteorol. Clim., 50, 1255–1274, 2011.
- 25 Kim, S.-Y. and Chun, H.-Y.: Stratospheric gravity waves generated by Typhoon Saomai (2006): numerical modeling in a moving frame following the typhoon, J. Atmos. Sci., 67, 3617–3636, doi:10.1175/2010JAS3374.1, 2010.
- Kim, S.-Y. and Chun, H.-Y.: Impact of typhoon-generated gravity waves in the typhoon development, Geophys. Res. Lett., 38, L01806, doi:10.1029/2010GL045719, 2011.

- Kim, S.-Y., Chun, H.-Y., and Baik, J.-J.: A numerical study of gravity waves induced by convection associated with Typhoon Rusa, *Geophys. Res. Lett.*, 32, L24816, doi:10.1029/2005GL024662, 2005.
- Kossin, J. P.: Daily hurricane variability inferred from GOES infrared imagery, *Mon. Weather Rev.*, 130, 2260–2270, 2002.
- Kuester, M. A., Alexander, M. J., and Ray, E. A.: A model study of gravity waves over Hurricane Humberto (2001), *J. Atmos. Sci.*, 65, 3231–3246, 2008.
- Merrill, R. T.: Environmental influences on hurricane intensification, *J. Atmos. Sci.*, 45, 1678–1687, 1988.
- Rappin, E. D., Morgan, M. C., Tripoli, G. J.: The impact of outflow environment on tropical cyclone intensification and structure, *J. Atmos. Sci.*, 68, 177–194, 2011.
- Weatherford, C. L. and Gray, W. M.: Typhoon structure as revealed by aircraft reconnaissance, Part I: Data analysis and climatology, *Mon. Weather Rev.*, 116, 1032–1043, 1988.
- Yoshioka, M. K., Kurihara, Y., and Ohfuchi, W.: Effect of the thermal tidal oscillation of the atmosphere on tropical cyclones, *Geophys. Res. Lett.*, 32, L16802, doi:10.1029/2005GL022716, 2005.

Horizontal divergence of typhoon-generated gravity waves

S. H. Kim et al.

[Title Page](#)

[Abstract](#)

[Introduction](#)

[Conclusions](#)

[References](#)

[Tables](#)

[Figures](#)

◀

▶

[Back](#)

[Close](#)

[Full Screen / Esc](#)

[Printer-friendly Version](#)

[Interactive Discussion](#)



Horizontal divergence of typhoon-generated gravity waves

S. H. Kim et al.

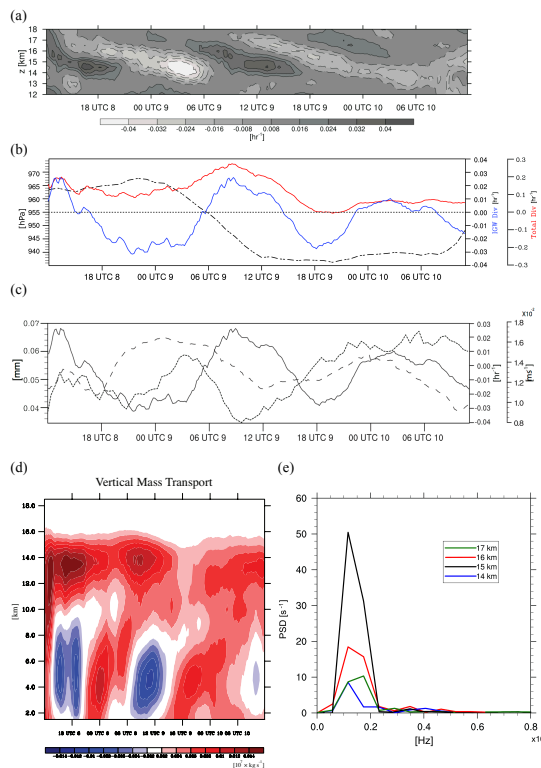


Fig. 1. (a) Time-height cross section of the domain-averaged HDTGW from 12 to 18 km a.g.l. Dashed and solid lines denote negative (convergence) and positive (divergence) values, respectively. (b) Time series of total divergence at 16 km a.g.l. (red), HDTGW (blue) and minimum sea-level pressure (dot dashed). (c) Time series of HDTGW at 16 km a.g.l. (solid), domain-averaged vertical velocity averaged over 3 to 15 km a.g.l. (dashed), and domain-averaged 30 min accumulated precipitation amount (dotted). (d) Time-height cross section of the vertical mass transport. (e) The power spectral density (PSD) of the HDTGW with respect to frequency at selected heights from 14 to 17 km a.g.l.

Horizontal divergence of typhoon-generated gravity waves

S. H. Kim et al.

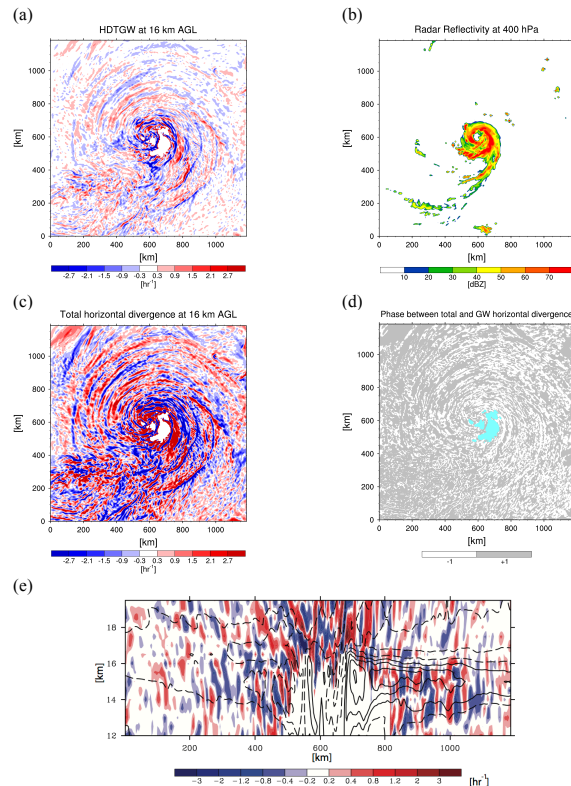


Fig. 2. (a) HDTGW at 16 km a.g.l., (b) radar reflectivity at 400 hPa, (c) total horizontal divergence at 16 km a.g.l. at 03:00 UTC 09, and (d) phase difference between the total horizontal divergence and HDTGW shown in (a) and (c). In (d), gray and white regions denote in phase and out of phase between (a) and (c), respectively, and blue color denotes cloud-covering area that corresponds to the white area shown in (a) and (c). (e) x - z cross section of zonal wind (contour) superimposed on HDTGW (shaded) at $y = 600$ km on 03:00 UTC 9. In (e), solid and dashed contours denote positive and negative values, respectively, with 5 ms^{-1} intervals.

Horizontal divergence of typhoon-generated gravity waves

S. H. Kim et al.

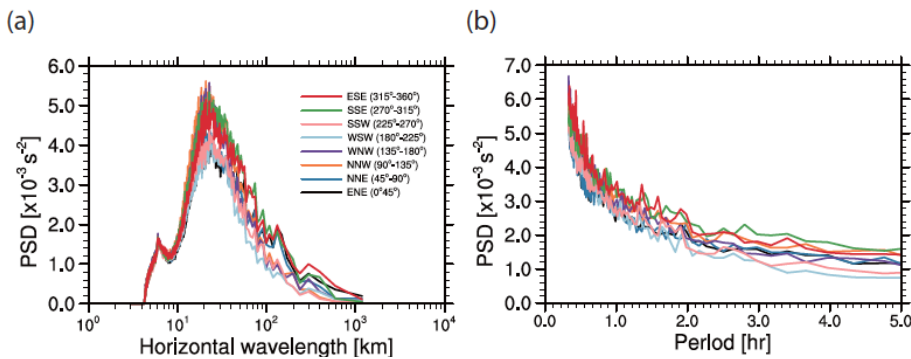


Fig. 3. PSDs of the HDTGW with respect to the (a) horizontal wavelength and (b) period in each propagation direction with 45° intervals at 16 km a.g.l.

Horizontal divergence of typhoon-generated gravity waves

S. H. Kim et al.

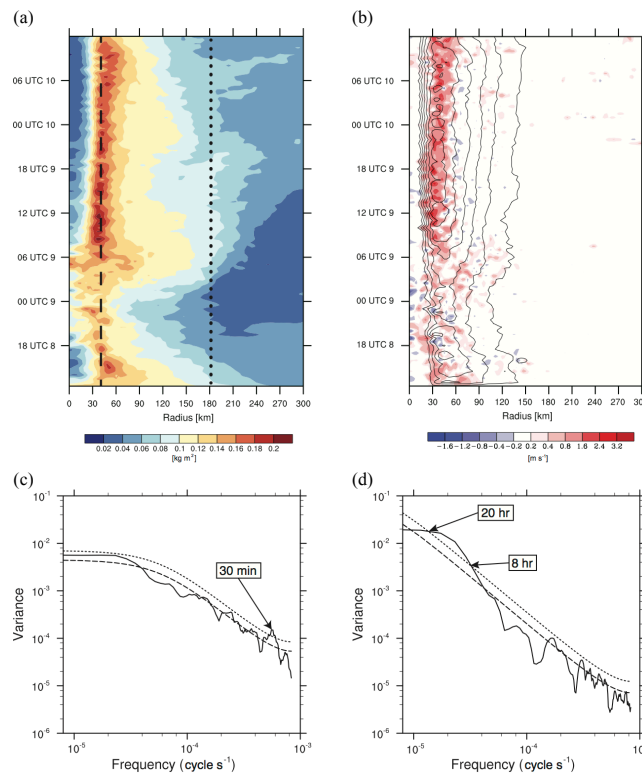


Fig. 4. (a) Hovmöller diagram of azimuthally averaged precipitable water (PW) in the simulation of typhoon Saomai. Dashed and dotted lines in (a) denote locations of spectral analyses performed in (c) and (d), respectively. (b) The same as in (a) except for the vertical velocity (color) at 1.5 km a.g.l. superimposed on the horizontal wind speed at 1.5 km a.g.l. from 25 to 50 m s⁻¹ with 5 m s⁻¹ intervals. The power spectrum of PW with respect to frequency are shown at (c) 40 km and (d) 180 km from the typhoon center. Dashed and dotted lines in (c) and (d) represent red noise and the 95 % confidence level, respectively.

Horizontal divergence of typhoon-generated gravity waves

S. H. Kim et al.

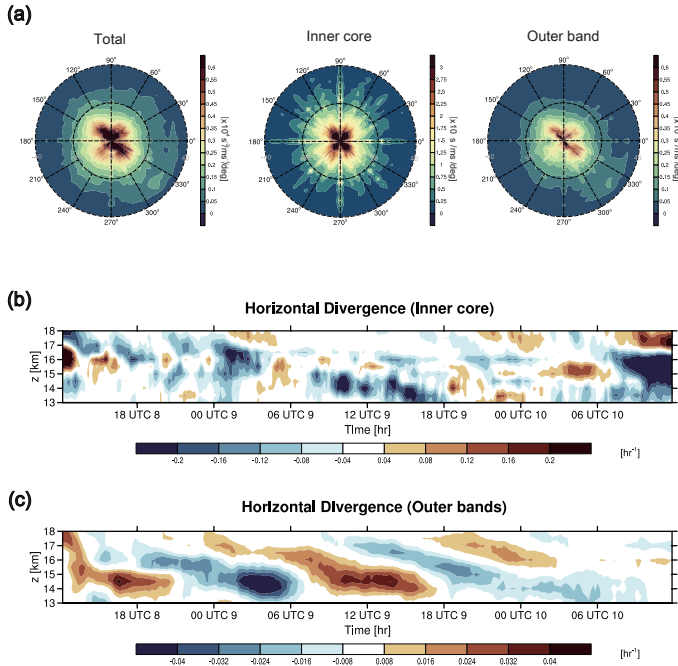


Fig. 5. (a) PSD of the HDTGW at 16 km a.g.l. with respect to the horizontal phase speed (radius) and propagation direction (azimuthal angle) in the total (left), inner core (middle), and outer rainbands (right) regions of D3. The inner core is defined by a 150 km radius from the typhoon center, and the outer rainbands region is defined by a region subtracting the inner core region from D3. Two dashed rings in each circle in (a) represent phase speeds of 20 and 40 ms⁻¹, respectively. Time-height cross sections of domain-averaged HDTGWs in the inner core and outer rainbands regions are shown in (b) and (c), respectively.

[Title Page](#)

[Abstract](#)

[Introduction](#)

[Conclusions](#)

[References](#)

[Tables](#)

[Figures](#)

◀

▶

[Back](#)

[Close](#)

[Full Screen / Esc](#)

[Printer-friendly Version](#)

[Interactive Discussion](#)